J|A|C|S
ARTICLES
Published on Web 03/21/2006

Benzonitrile Extrusion from Molybdenum(IV) Ketimide Complexes Obtained via Radical C−E (E = O, S, Se) Bond Formation: Toward a New Nitrogen Atom Transfer Reaction

Arjun Mendiratta,[†] Christopher C. Cummins,*[,†] Olga P. Kryatova,[‡] Elena V. Rybak-Akimova,*[,‡] James E. McDonough,[§] and Carl D. Hoff*[,§]

Contribution from the Department of Chemistry, Massachusetts Institute of Technology, 77 Massachusetts Avenue, Cambridge, Massachusetts 02139, Department of Chemistry, Tufts University, 62 Talbot Avenue, Medford, Massachusetts 02155, and Department of Chemistry, University of Miami, 1301 Memorial Drive, Coral Gables, Florida 33146

Received December 27, 2005; E-mail: ccummins@mit.edu

Abstract: Beta-elimination is explored as a possible means of nitrogen-atom transfer into organic molecules. Molybdenum(IV) ketimide complexes of formula (Ar[*t*-Bu]N)$_3$Mo(N═C(X)Ph), where Ar = 3,5-Me$_2$C$_6$H$_3$ and X = SC$_6$F$_5$, SeC$_6$F$_5$, or O$_2$CPh, are formally derived from addition of the carbene fragment [:C(X)Ph] to the terminal nitrido molybdenum(VI) complex (Ar[*t*-Bu]N)$_3$Mo≡N in which the nitrido nitrogen atom is installed by scission of molecular nitrogen. Herein the pivotal (Ar[*t*-Bu]N)$_3$Mo(N═C(X)Ph) complexes are obtained through independent synthesis, and their propensity to undergo beta-X elimination, i.e., conversion to (Ar[*t*-Bu]N)$_3$MoX + PhC≡N, is investigated. Radical C−X bond formation reactions ensue when benzonitrile is complexed to the three-coordinate molybdenum(III) complex (Ar[*t*-Bu]N)$_3$Mo and then treated with 0.5 equiv of X$_2$, leading to facile assembly of the key (Ar[*t*-Bu]N)$_3$Mo(N═C(X)Ph) molecules. Treated herein are synthetic, structural, thermochemical, and kinetic aspects of (i) the radical C−X bond formation and (ii) the ensuing beta-X elimination processes. Beta-X elimination is found to be especially facile for X = O$_2$CPh, and the reaction represents an attractive component of an overall synthetic cycle for incorporation of dinitrogen-derived nitrogen atoms into organic nitrile (R−C≡N) molecules.

Introduction

The utilization of molecular nitrogen as an N-atom source in synthesis,[1−4] both as a societal goal and as a challenge to modern chemistry,[5,6] can potentially be achieved through the development of methods for transfer of N$_2$-derived nitrido nitrogen atoms to appropriate acceptor compounds.[7] This is so in part because now are known several early d-block element systems capable of dinitrogen reductive scission[8−19] to produce the nitridometal (M≡N) functional group[20,21] in either its terminal or bridging bonding modes. Simple derivatization with an electrophile (e.g., trifluoroacetic anhydride, TFAA) is a typical method of activation of the nitridometal functional group toward an acceptor substrate,[22,23] and it is a process in which the metal oxidation state remains fixed (Scheme 1a). An alternative would be derivatization with a redox-active agent as in the case of carbene addition to the terminal nitridometal functional group as shown in Scheme 1b.

An attractive N-atom transfer scheme that involves carbene-to-nitrido addition as the N−C bond-forming step (Scheme 1b) is that in which subsequent beta-elimination of the group X to the metal center releases the nitrile R−C≡N in its free form. In appealing fashion, this hypothetical sequence of events exchanges a metal−nitrogen for a carbon−nitrogen triple bond.

[†] Massachusetts Institute of Technology.
[‡] Tufts University.
[§] University of Miami.

(1) Mori, M. *J. Organomet. Chem.* **2004**, *689*, 4210−4227.
(2) Mori, M.; Akashi, M.; Hori, M.; Hori, K.; Nishida, M.; Sato, Y. *Bull. Chem. Soc. Japan* **2004**, *77*, 1655−1670.
(3) Hidai, M.; Ishii, Y. *J. Mol. Catal. A: Chem.* **1996**, *107*, 105−112.
(4) Hidai, M.; Ishii, Y. *Bull. Chem. Soc. Japan* **1996**, *69*, 819−31.
(5) Lippard, S. J. *Chem. Eng. News* **2000**, *78*, 64−65.
(6) Smaglik, P. *Nature* **2000**, *406*, 807−808.
(7) Henderickx, H.; Kwakkenbos, G.; Peters, A.; van der Spoel, J.; de Vries, K. *Chem. Commun.* **2003**, 2050−2051.
(8) Laplaza, C. E.; Cummins, C. C. *Science* **1995**, *268*, 861−863.
(9) Laplaza, C. E.; Johnson, M. J. A.; Peters, J. C.; Odom, A. L.; Kim, E.; Cummins, C. C.; George, G. N.; Pickering, I. J. *J. Am. Chem. Soc.* **1996**, *118*, 8623−8638.
(10) Peters, J. C.; Cherry, J. P. F.; Thomas, J. C.; Baraldo, L.; Mindiola, D. J.; Davis, W. M.; Cummins, C. C. *J. Am. Chem. Soc.* **1999**, *121*, 10053−10067.
(11) Mindiola, D. J.; Meyer, K.; Cherry, J. P. F.; Baker, T. A.; Cummins, C. C. *Organometallics* **2000**, *19*, 1622−1624.
(12) Tsai, Y. C.; Cummins, C. C. *Inorg. Chim. Acta* **2003**, *345*, 63−69.
(13) Sceats, E. L.; Figueroa, J. S.; Cummins, C. C.; Loening, N. M.; Van der Wel, P.; Griffin, R. G. *Polyhedron* **2004**, *23*, 2751−2768.
(14) Zanotti-Gerosa, A.; Solari, E.; Giannini, L.; Floriani, C.; Chiesi-Villa, A.; Rizzoli, C. *J. Am. Chem. Soc.* **1998**, *120*, 437−438.
(15) Caselli, A.; Solari, E.; Scopelliti, R.; Floriani, C.; Re, N.; Rizzoli, C.; Chiesi-Villa, A. *J. Am. Chem. Soc.* **2000**, *122*, 3652−3670.
(16) Solari, E.; Da Silva, C.; Iacono, B.; Hesschenbrouck, J.; Rizzoli, C.; Scopelliti, R.; Floriani, C. *Angew. Chem., Int. Ed.* **2001**, *40*, 3907−3909.
(17) Clentsmith, G. K. B.; Bates, V. M. E.; Hitchcock, P. B.; Cloke, F. G. N. *J. Am. Chem. Soc.* **1999**, *121*, 10444−10445.
(18) Bates, V. M. E.; Clentsmith, G. K. B.; Cloke, F. G. N.; Green, J. C.; Jenkin, H. D. L. *Chem. Commun.* **2000**, 927−928.
(19) Kawaguchi, H.; Matsuo, T. *Angew. Chem., Int. Ed.* **2002**, *41*, 2792−2794.
(20) Dehnicke, K.; Strähle, J. *Angew. Chem., Int. Ed.* **1992**, *31*, 955−978.
(21) Eikey, R. A.; Abu-Omar, M. M. *Coord. Chem. Rev.* **2003**, *243*, 83−124.
(22) DuBois, J.; Tomooka, C. S.; Hong, J.; Carreira, E. M. *Acc. Chem. Res.* **1997**, *30*, 364−372.
(23) Groves, J. T.; Takahashi, T. *J. Am. Chem. Soc.* **1983**, *105*, 2073−2074.

Scheme 1

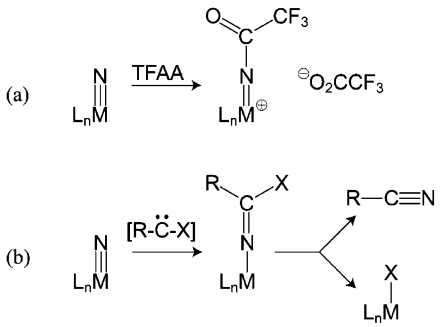

Toward the realization of such a sequence, herein we take advantage of independent synthesis to access complexes of the sort $L_nM-N=C(X)R$.[24] Of key import is the identification of groups X that do in fact undergo facile beta-elimination, producing L_nMX and evolving the organic nitrile R−C≡N.

The three-coordinate molybdenum(III) complex Mo(N[*t*-Bu]-Ar)$_3$ (**1**, Ar = 3,5-$Me_2C_6H_3$) is active for the six-electron reductive scission of molecular nitrogen under exceedingly mild conditions and in homogeneous solution.[8−10,12,13] Thereby is produced the terminal nitrido complex N≡Mo(N[*t*-Bu]Ar)$_3$, **2**. Its isotopomer ^{15}N≡Mo(N[*t*-Bu]Ar)$_3$ (**2**-^{15}N), available in high yield from $^{15}N_2$, may find application as an ^{15}N-labeling reagent if suitable nitrogen-atom transfer chemistries can be discovered.[25] New stoichiometric chemical reactions for nitrogen-atom transfer, such as the beta-elimination idea probed herein (Scheme 1b, second step), should also be considered as potential components of new *catalytic* nitrogen-atom transfer cycles.

We have shown previously that a two-step sequence of methylation and dehydrohalogenation delivers methylene to nitrido complex **2** to generate the structurally characterized parent molybdenum(IV) ketimide derivative (Ar[*t*-Bu]N)$_3$Mo−N=CH_2 (Scheme 2, top).[13] The latter result demonstrates that it is indeed possible to obtain by formal carbene addition to nitride complex **2** an isolable molybdenum(IV) ketimide complex. The more complicated ketimide derivatives (Ar[*t*-Bu]N)$_3$Mo−N=C(X)Ph (**3a**−**f**, X = TePh, SC_6F_5, SeC_6F_5, O_2CPh, SPh, and SePh, respectively) of the type required for the present study, are generated instead through a fascinating radical C−X bond-forming process. The synthesis and structural characterization of the thermally robust X = SPh and SePh derivatives **3e** and **3f** were communicated recently, together with the first observation of beta-X elimination in such a molecule, the X = TePh derivative **3a** which extrudes PhCN to yield the molybdenum(IV) phenyltellurolate complex (Ar[*t*-Bu]N)$_3$Mo−TePh, **4a**.[24]

The radical C−X bond-forming process leading to **3a**−**f** is a consequence of radical character conferred upon the nitrile carbon atom upon formation of the benzonitrile adduct **5**, as shown in Scheme 2. This paper discusses the structure and properties of radical adduct **5** and its key role in the synthesis of **3a**−**f** as well as the detailed investigation of the mechanism and energetics of nitrile extrusion.

Experimental Section

General Considerations. Unless stated otherwise, all operations were performed in a Vacuum Atmospheres or MBraun drybox under an atmosphere of purified nitrogen or argon. Anhydrous diethyl ether was purchased from Mallinckrodt; pentane, *n*-hexane, and tetrahydrofuran (THF) were purchased from EM Science. Diethyl ether, toluene, benzene, pentane, and *n*-hexane were dried and deoxygenated by the method of Grubbs.[26] THF was distilled under nitrogen from purple sodium benzophenone ketyl. Distilled solvents were transferred under vacuum into vacuum-tight glass vessels before being transferred into a Vacuum Atmospheres drybox. C_6D_6 was purchased from Cambridge Isotopes and was degassed and dried over 4 Å sieves. THF-d_8 was passed through a column of activated alumina and stored over 4 Å sieves. The 4 Å sieves, alumina, and Celite were dried in vacuo overnight at a temperature just above 200 °C. Compounds **1**,[9,27] the amine HN(*t*-Bu)Ar[28] and $MoCl_3(THF)_3$[29] required for its synthesis, $(C_6F_5S)_2$,[30] and $(C_6F_5Se)_2$[31] were prepared following literature methods. PhCN was distilled under reduced pressure before use and stored in a nitrogen-filled drybox. All other compounds were used as received. ^{1}H and ^{13}C NMR spectra were recorded on Unity 300, Mercury 300, or Varian INOVA-501 spectrometers at room temperature, unless indicated otherwise. ^{13}C NMR spectra are proton decoupled. Chemical shifts are reported with respect to internal solvent: 7.16 ppm and 128.38 (t) ppm (C_6D_6). ^{77}Se NMR spectra were recorded on a Varian INOVA-501 spectrometer and are referenced to Me_2Se (0 ppm) by comparison to external Se_2Ph_2 ($CDCl_3$, 460 ppm). UV−vis absorption spectra were collected on a HP 8452A diode array spectrometer fitted with an HP 89090A Peltier temperature controller. CHN analyses were performed by H. Kolbe Mikroanalytisches Laboratorium (Mülheim, Germany).

Scheme 2

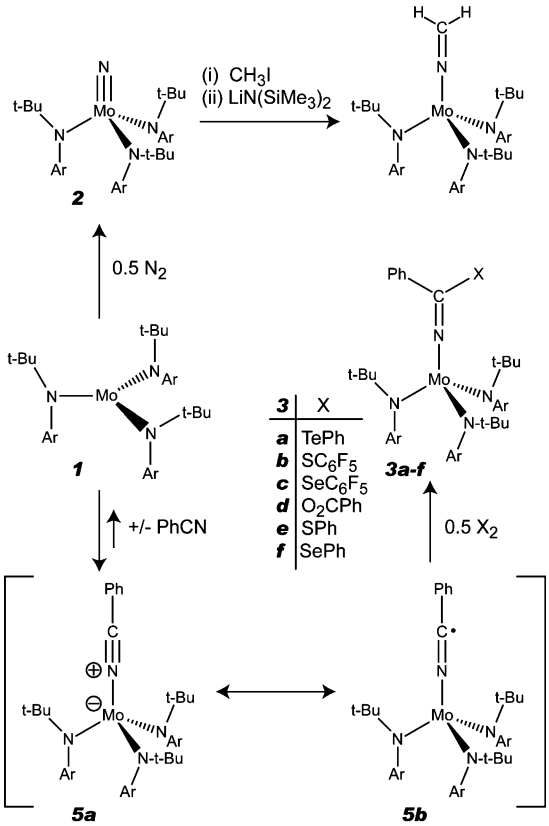

(24) Mendiratta, A.; Cummins, C. C.; Kryatova, O. P.; Rybak-Akimova, E. V.; McDonough, J. E.; Hoff, C. D. *Inorg. Chem.* **2003**, *42*, 8621−8623.
(25) Chisholm, M. H.; Delbridge, E. E.; Kidwell, A. R.; Quinlan, K. B. *Chem. Commun.* **2003**, 126−127.
(26) Pangborn, A. B.; Giardello, M. A.; Grubbs, R. H.; Rosen, R. K.; Timmers, F. J. *Organometallics* **1996**, *15*, 1518−1520.
(27) Laplaza, C. E.; Odom, A. L.; Davis, W. M.; Cummins, C. C.; Protasiewicz, J. D. *J. Am. Chem. Soc.* **1995**, *117*, 4999−5000.
(28) Tsai, Y. C.; Stephens, F. H.; Meyer, K.; Mendiratta, A.; Gheorghiu, M. D.; Cummins, C. C. *Organometallics* **2003**, *22*, 2902−2913.
(29) Stoffelbach, F.; Saurenz, D.; Poli, R. *Eur. J. Inorg. Chem.* **2001**, 2699−2703.
(30) McKillop, A.; Koyuncu, D.; Krief, A.; Dumont, W.; Renier, P.; Trabelsi, M. *Tetrahedron Lett.* **1990**, *31*, 5007.
(31) Klapötke, T. M.; Krumm, B.; Polborn, K. *Eur. J. Inorg. Chem.* **1999**, 1359−1366.

Synthesis of 3b. In a 50-mL round-bottom flask was prepared a solution of **1**−NCPh (600 mg **1**, 100 mg PhCN, 0.96 mmol) in 20 mL of Et_2O. To the purple solution was added solid $(C_6F_5S)_2$ (192 mg, 0.48 mmol), resulting in a rapid darkening to deep blue. The reaction mixture was allowed to stir for 5 min, whereupon it was filtered and concentrated to dryness. Recrystallization from Et_2O furnished product **3b** as a dark, microcrystalline solid. Yield: 503 mg, 0.54 mmol (3 crops, 56%). ^{1}H NMR (300 MHz, C_6D_6): δ 1.32 (br s, 27H, C*Me*$_3$); 2.25 (s, 18H, C_6H_3*Me*$_2$); 6.57 (s, 2H, phenyl ortho); 6.63 (t, 1H, phenyl para); 6.69 (s, 3H, Ar para); 6.91 (s, 6H, Ar ortho); 7.01 (t, 2H, phenyl meta). ^{19}F NMR (282 MHz, C_6D_6): δ −135.43 (dd); −156.71 (t); −163.02 (m). UV−vis (Et_2O, 25 °C): λ_{max} 318 (sh, ϵ = 19000 $M^{-1}cm^{-1}$); 577 (ϵ = 7800 $M^{-1}cm^{-1}$) nm. The thermal instability of this compound precluded satisfactory elemental analysis and ^{13}C NMR data.

Generation and Spectroscopic Observation of 3c. A solution of **1** (17 mg, 0.027 mmol) and PhCN (ca. 5 mg, 0.49 mmol) was prepared in 0.5 mL of C_6D_6. To this was added a solution of $(C_6F_5Se)_2$ (7 mg, 0.014 mmol) in 0.5 mL of C_6D_6, resulting in an immediate color change to deep blue. The mixture was rapidly transferred to a J. Young NMR tube which was then removed from the glovebox and frozen in an ice bath while being transported to the NMR spectrometer. The very first ^{1}H NMR spectrum that is obtained shows a 10:1 mixture of **3c** and **4c**. Over the course of 30 min, the signals corresponding to **3c** are observed to decay, and those corresponding to **4c** grow in. ^{1}H NMR (300 MHz, C_6D_6): δ 1.29 (br s, 27H, C*Me*$_3$); 2.27 (s, 18H, C_6H_3*Me*$_2$); 6.73 (3H, Ar para); 6.85 (6H, Ar ortho); 7.03 (t, 2H, phenyl meta) (other resonances obscured). UV−vis (Et_2O, 25 °C): λ_{max} 579 (ϵ = 5500 $M^{-1}cm^{-1}$) nm.

Synthesis of 4b. To an Et_2O solution of **1** (200 mg, 0.32 mmol) was added an Et_2O solution of $(C_6F_5S)_2$ (64 mg, 0.16 mmol), resulting in a color change to purple-brown upon mixing. The solution was filtered through Celite, and the filtrate so obtained was concentrated to dryness. Recrystallization from Et_2O (−35 °C) furnished 150 mg (0.18 mmol, 57%) of dark crystalline material. ^{1}H NMR (300 MHz, C_6D_6): δ 1.39 (s, 27H, C*Me*$_3$); 2.05 (s, 18H, C_6H_3*Me*$_2$); 6.25 (br s, 6H, Ar ortho); 6.39 (s, 3H, Ar para). ^{19}F NMR (282 MHz, C_6D_6): δ −131.33 (dd); −159.66 (t); −163.78 (m). ^{13}C NMR: δ 21.61 (C_6H_3*Me*$_2$); 31.73 (C*Me*$_3$); 63.31 (N−*C*Me$_3$); 127.09; 129.03; 132.41 (m, *C*−F); 136.15; 136.68 (m, *C*−F); 140.19 (m, *C*−F); 143.63 (m, *C*−F); 146.81 (m, *C*−F); 151.58. UV−vis (Et_2O, 25 °C): λ_{max} 389 (sh, ϵ = 4500 $M^{-1}cm^{-1}$); 563 (ϵ = 1900 $M^{-1}cm^{-1}$) nm. Anal. Calcd for $C_{42}H_{54}N_3MoSF_5$: C, 61.23; H, 6.61; N, 5.10. Found: C, 60.95; H, 6.68; N, 5.04.

Synthesis of 4c. Synthesized analogously to **4b**. Yield: 150 mg, 0.17 mmol, 54%. ^{1}H NMR (300 MHz, C_6D_6): δ 1.40 (s, 27H, C*Me*$_3$); 2.04 (s, 18H, C_6H_3*Me*$_2$); 6.21 (br s, 6H, Ar ortho); 6.38 (s, 3H, Ar para). UV−vis (Et_2O, 25 °C): λ_{max} 387 (sh, ϵ = 5500 $M^{-1}cm^{-1}$); 555 (ϵ = 1900 $M^{-1}cm^{-1}$) nm. Anal. Calcd for $C_{42}H_{54}N_3MoSeF_5$: C, 57.93; H, 6.25; N, 4.83. Found: C, 57.79; H, 6.08; N, 4.78.

Spectroscopic Observation of 3d. A J. Young NMR tube was charged with **1** (24 mg, 0.038 mmol), PhCN (9 mg, 0.087 mmol), and 0.4 mL of toluene-d_8. The resulting purple solution was frozen in the glovebox coldwell. To the frozen purple solution was then added benzoyl peroxide (5 mg, 0.020 mmol) in 0.4 mL of toluene-d_8, after which the contents of the NMR tube were frozen completely. The NMR tube was quickly removed from the glovebox and transferred to a dry ice/acetone bath where it was allowed to thaw with gentle shaking to ensure good mixing of the reagents. The NMR tube was maintained at −78 °C before being transferred to an NMR probe precooled to −15 °C. A ^{1}H NMR spectrum was taken as soon as thermal equilibration was obtained. Subsequent spectra were taken in order to monitor the smooth conversion of **3d** to **4d** and PhCN. ^{1}H NMR (500 MHz, toluene, −15 °C): δ 1.29 (s, 9H, C*Me*$_3$); 1.33 (s, 18H, C*Me*$_3$); 2.14 (s, 6H, C_6H_3*Me*$_2$); 2.39 (s, 12H, C_6H_3*Me*$_2$); 8.31 (1H, d, phenyl para) (other aryl resonances obscured).

Synthesis of 4d. A purple solution of **1** (200 mg, 0.32 mmol) and PhCN (33 mg, 0.32 mmol) in 5 mL of Et_2O was cooled until frozen and then allowed to thaw. To the thawing solution was added a room-temperature solution of benzoyl peroxide (39 mg, 0.16 mmol) in Et_2O (2 mL). As the reaction mixture was allowed to warm to room temperature, the initial purple color was observed to become blue and then purple again. Stirring was continued for an additional 5 min, at which point the reaction mixture was filtered through Celite, and the filtrate so obtained was concentrated to dryness. Recrystallization from Et_2O furnished **4d** as large brown crystals. Yield: 169 mg, 0.22 mmol (2 crops, 71%). ^{1}H NMR (500 MHz, C_6D_6): δ 1.68 (s, 18H, C_6H_3*Me*$_2$); 3.98 (br s, 27H, C*Me*$_3$); 4.87 (s, 3H, Ar para); 5.64 (s, 6H, Ar meta); 6.20 (t, 1H, phenyl para); 7.27 (poorly resolved t, 2H, phenyl meta); 7.58 (poorly resolved d, 2H, phenyl ortho). Anal. Calcd for $C_{43}H_{59}N_3O_2$-Mo: C, 69.24; H, 7.97; N, 5.63. Found: C, 68.95; H, 8.11; N, 5.55.

Kinetic Measurements. Kinetics of β-EC_6F_5 elimination from **3b** (E = S) and **3c** (E = Se) were measured using UV−vis spectroscopy over a 40 °C range (E = S, 25−65 °C; E = Se, 15−55 °C). For **3b**, ca. 0.1 mM solutions in THF were prepared from freshly crystallized material and then transferred to a quartz UV cell containing a micro stirbar. For **3c**, an identical protocol was followed, except that the more rapid kinetics in this system required that the starting ketimide be generated in situ. In all cases, very good fits to the first-order kinetic equation were obtained. In addition, rate constants obtained from traces at three different wavelengths (400, 475, 585 nm) were within 10% of each other. The kinetic data are summarized in Tables S1 and S2.

Stopped-Flow Kinetic Measurements. Toluene solutions of the reagents were prepared in a Vacuum Atmospheres or an MBraun glovebox filled with argon and placed in Hamilton gas-tight syringes. Time-resolved spectra were acquired at temperatures from −80 to −40 °C using a Hi-Tech Scientific (Salisbury, Wiltshire, UK) SF-43 Multi-Mixing CryoStopped-Flow Instrument in a diode array mode. Control kinetic experiments in the systems that did not contain benzoyl peroxide used a powerful xenon arc lamp. All kinetic experiments with benzoyl peroxide were done with a low-power visible lamp to prevent decomposition of peroxide induced by UV light.[32]

The stopped-flow instrument was equipped with stainless steel plumbing, a 1.00-cm stainless steel mixing cell with sapphire windows, and an anaerobic gas-flushing kit. The instrument was connected to an IBM computer with IS-2 Rapid Kinetic software (Hi-Tech Scientific). The temperature in the mixing cell was maintained to ±0.1 K, and the mixing time was 2 to 3 ms. The driving syringe compartment and the cooling bath filled with heptane (Fisher) were flushed with argon before and during the experiments, using anaerobic kit flush lines. All flow lines of the SF-43 instrument were extensively washed with degassed, anhydrous toluene before charging the driving syringes with reactant solutions.

All of the experiments were performed in a single-mixing mode of the instrument, with a 1:1 (v/v) ratio. The system was studied using two mixing approaches: (1) first syringe, complex **1**; second syringe, premixed PhCN and benzoyl peroxide and (2) first syringe, premixed complex **1** and PhCN; second syringe, benzoyl peroxide.

In both mixing conditions the concentration of the reagents were varied: complex **1** (0.3−0.225 mM), PhCN (0.3−3 mM), benzoyl peroxide (0.15−3.6 mM).

Under both mixing conditions, consistent and reproducible results were obtained, and the formation of the ketimide complex intermediate **3d** was observed.

Spectral changes and reaction rates in control experiments (mixing of complex **1** with PhCN, and mixing of complex **1** with benzoyl peroxide) were distinct from those observed in the ternary system (**1** + excess PhCN + benzoyl peroxide).

The reactions were monitored for 3−5 half-lives. A series of 4−6 measurements at each temperature gave an acceptable standard deviation

(32) Bradley, J. D.; Roth, A. P. *Tetrahedron Lett.* **1971**, 3907−10.

(within 10%). Data analysis was performed with IS-2 Rapid Kinetic software from Hi-Tech Scientific, Spectfit/32 Global Analysis System software from Spectrum Software Associates, or Excel Solver from Microsoft.

Calorimetric Measurements. Enthalpies of reaction were measured using a rapid response solution calorimeter designed for anaerobic use. The vessel was constructed by Ace Glass and includes six ace threaded seal fittings fitted to a 350-mL reactor which is sealed inside an evacuated outer jacket to yield a thermally insulated system. In place of a stirrer, the vessel is attached to a special rocking device constructed from a modified autoclave rocker obtained from American Instruments. The calorimeter and assembly are in an air thermostated box. Three of the six threaded joints are fitted with ampule holders fixed to Teflon rods. A precision thermistor probe and resistance heater are sealed through two of the other Ace threaded ports. The final port is fitted to a high-vacuum stopcock attached via butyl rubber tubing to a Schlenk manifold.

In a typical procedure, a solution of 3.6 g of complex **1** in 200 mL of freshly distilled toluene was prepared in the glovebox in a Schlenk tube. The solution was then transferred under argon via stainless steel cannula. The calorimeter itself was evacuated and fitted with three ampules of PhSe−SePh sealed in fragile glass bulbs and containing 0.1028, 0.1020, and 0.1639 g. The system was sealed and allowed to come to near thermal equilibrium while the rocker was active. At that time 10 mL of distilled benzonitrile was added to the solution to generate **1**−NCPh in situ. This exothermic process returns to a stable baseline after about 10 minutes. Due to the slow dimerization of **1**−NCPh, reactions are studied quickly. The slow exothermic character of this dimerization is absorbed into the background of the calorimeter signal of both the reactions and the electrical calibrations and is judged to not interfere with the measurements of the rapid reactions. Following electrical calibration with the heater, the first of the three ampules is broken, and a second electrical calibration is performed. The second and third ampules are broken without an additional intervening electrical calibration, and then two additional electrical calibrations are performed. The enthalpies of the three reactions are −39.76, −39.69, and −38.60 kcal/mol yielding a value of −39.4 ± 0.7 for the enthalpy of reaction of solid PhSe−SePh. This value is corrected for the enthalpy of solution of PhSe−SePh which was measured separately as 6.0 ± 0.2 kcal/mol to yield the final value in solution of −45.4 ± 0.9 kcal/mol of PhSe−SePh in the reaction: 2 **1**−NCPh + PhSe−SePh → 2 **3e**. Data reported in Figure 7 correspond to 1/2 this value since they are per mole of **3**−NCPh. Corresponding reactions of PhS−SPh and BzOOBz were carried out at ambient temperature, and also the enthalpies of solution of 6.1 ± 0.1 (PhSSPh) and 5.1 ± 0.4 (BzOOBz) kcal/mol have been incorporated into data in Scheme 7.

Data for the reaction of **3**−NCPh and benzoyl peroxide at −25 °C were obtained using similar techniques as those described above. In this case, however, the entire calorimetric system was mounted in a General Technology Corporation evacuable glovebox. A constant-temperature alcohol bath maintained at −30 °C was pumped through the sealed fitting in the wall of the glovebox such that both the external jacket of the calorimeter and a special sealed copper insertion probe were maintained at −30 °C. Following loading of the calorimeter with a solution of complex **1**, the copper probe is inserted into one of the fittings of the insulated calorimeter vessel, allowing rapid lowering of the temperature to −30 °C. At that time the probe is removed, 10 mL of PhCN is added to produce in situ **3**−NCPh, and the ampule holder assembly is added to replace the low-temperature probe. Because of the slow-temperature rise due to both the electrical calibrations and the exothermic reaction of benzoyl peroxide, the average temperature of the reaction was ca. −25 °C for the measurements. On the basis of five individual measurements the experimental data yield −105.5 ± 4.2 kcal/mol of benzoyl peroxide. As discussed above, these data yield a value, reported in Figure 7, of −55.3 ± 2.3 kcal/mol adjusted for the enthalpy of solution of benzoyl peroxide and divided by two to correspond to the enthalpy of reaction per mole of **3**−NCPh.

Table 1. Crystallographic Data for Compounds **3b**, **4b**, and **4c**

	3b	4b	4c
formula	$C_{49}H_{59}F_5MoN_4S$	$C_{42}H_{54}F_5MoN_3S$	$C_{43}H_{50}MoN_3O_2$
FW	927.00	823.88	736.80
space group	$P-1$	$P2_1/c$	$P-1$
a, Å	10.6395(10)	11.0092(6)	10.8341(11)
b, Å	12.8842(14)	18.7121(11)	19.982(2)
c, Å	18.843(2)	20.1675(11)	20.569(2)
α, deg	70.329(4)	90.00	89.669(2)
β, deg	74.155(3)	110.5280(10)	81.701(2)
γ, deg	76.599(3)	90.00	75.221(2)
V, Å^3	2311.8(4)	4003.0(4)	4258.2(7)
Z	4	4	4
D, g/cm^3	1.332	1.367	1.221
μ, Mo Kα, mm^{-1}	0.387	0.436	0.347
temp, K	100	173	193
F(000)	968	1720	1548
GoF(F^2)	1.057	1.201	1.024
R(F), %	0.0371	0.0827	0.0322
wR(F), %	0.0865	0.1386	0.0864

FTIR Kinetic Studies. Kinetic studies of benzonitrile elimination from in situ generated **3d** yielding molybdenum(IV) benzoate complex **4d** were performed using a Perkin-Elmer System 2000 FTIR spectrometer equipped with an MCT detector. Reactions were performed in a thermostated vessel under an argon atmosphere. The vessel contained ports for direct insertion of a Pt RTD precision thermometer, a stopcock protected septum inlet, a sealed thread assembly allowing a 1/8 in.-thick wall Teflon tubing to connect directly to a flow-through cell micro FTIR cell obtained from Harrick Scientific. The cell and reactor assembly were mounted in a thick-walled polycarbonate box which fits in the spectrometer base of the PE 2000 FTIR and contains two CaF_2 windows fitted with argon purge to eliminate condensation at low temperature. The external coolant controls the temperature of both the reactor, the cell, and the lines inside the box, all of which are thermostated to the same temperature.

In a typical procedure a solution 0.5 g of **1** in 30 mL of toluene is allowed to equilibrate at 1.3 °C. Following equilibration, 2 mL of PhCN is added to generate **3**−NCPh in situ, and an FTIR is recorded. Following injection of a solution of 0.093 g of recrystallized benzoyl peroxide in 1 mL of toluene to generate ketimide **3d**, the reaction is monitored periodically by withdrawing a sample from the reactor to the cell. Typical spectroscopic data are shown in Figure 5 of the text, where the decrease of the band at 1730 cm^{-1} assigned to ν(C═O) of **3d** is balanced by the increase in the band at 1660 cm^{-1} assigned to ν(C═O) of benzoate **4d**. A plot of ln($A - A_\infty$) was found to be linear through more than three half-lives as shown in Figure S1 (see Supporting Information [SI]). Values of the first-order rate constants (s^{-1}) were as follows: 0.0277 (10.3 °C), 0.0132 (4 °C), 0.0087 (1.2 °C), 0.00102 (−12 °C), 0.00011 (−30 °C). These data are shown in the Eyring plot, Figure S2, and yield activation parameters $\Delta H^\ddagger = 18.6$ kcal/mol and $\Delta S^\ddagger = -0.1$ cal mol^{-1} K^{-1}.

Crystallographic Structure Determinations. Crystals were grown from saturated Et_2O solutions at −35 °C. The X-ray crystallographic data collections were carried out on a Siemens Platform three-circle diffractometer mounted with a CCD or APEX-CCD detector and outfitted with a low-temperature, nitrogen-stream aperture. The structures were solved using direct methods, in conjunction with standard difference Fourier techniques and refined by full-matrix least-squares procedures. A summary of the crystallographic data for complexes **3b**, **4b**, and **4c** is shown in Table 1. An empirical absorption correction (either ψ-scans or SADABS) was applied to the diffraction data for all structures. All non-hydrogen atoms were refined anisotropically. Unless otherwise specified, all hydrogen atoms were treated as idealized contributions and refined isotropically. All software used for diffraction

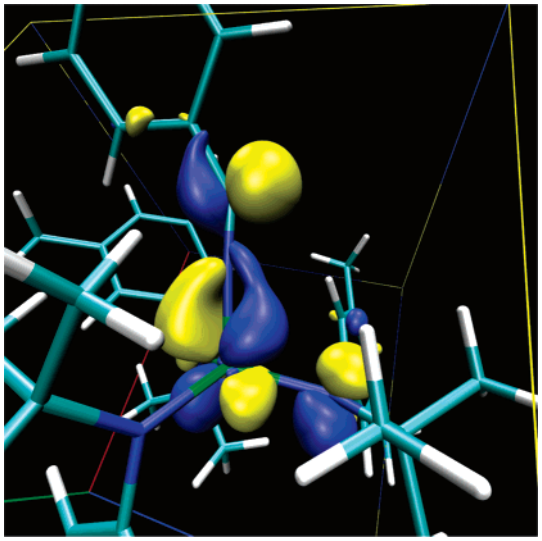

Figure 1. SOMO of computational model **5miii**.

data processing and crystal-structure solution and refinement are contained in the SAINT+ (v6.45) and SHELXTL (v6.14) program suites, respectively (G. Sheldrick, Bruker AXS, Madison, WI).

Results and Discussion

Structure of Benzonitrile Adduct 5. The reactive intermediate in our present synthesis of molybdenum(IV) ketimide complexes is the odd-electron benzonitrile adduct **5** of the three-coordinate complex **1**. In prior work we had invoked the η^1-benzonitrile bonding mode as the reactive form, taking the position that the alternative η^2-bound form of the system—analogous to the crystallographically determined structure of dimethylcyanamide adduct (Ar[*t*-Bu]N)$_3$Mo(η^2-NCNMe$_2$)[28]—would be the more stable isomer.[24,28] For the present work we have carried out full-molecule geometry optimizations on **5** using DFT computational methods (see SI for full details). Three initial models were considered: (i) an η^2 model **5mi** based upon the crystal structure of (Ar[*t*-Bu]N)$_3$Mo(η^2-NCNMe$_2$) with PhCN replacing the η^2 dimethylcyanamide ligand, (ii) an η^1 model **5mii** based upon the crystal structure of the odd-electron oxo complex (Ar[*t*-Bu]N)$_3$Mo═O,[33] with NCPh replacing the oxo ligand, and (iii) an η^1 model **5miii** based upon the crystal structure of the structurally characterized[24] ketimide complex **3f** with deletion of the SePh substituent. The latter two models both incorporate η^1 bonding of the benzonitrile ligand but offer alternative conformations for the complement of three sterically demanding N(*t*-Bu)Ar ligands. Both of the η^1 model structures are slightly preferred over the η^2 structure, **5mii** by 4.3 and **5miii** by 1.0 kcal/mol.

The observed reactivity in the synthesis of **3a**−**f** is also suggestive of η^1-benzonitrile binding in intermediate adduct **5**, being that this bonding mode exposes the cyano carbon atom to external attack. Additionally, in this mode a cyano carbon p orbital contributes substantially to the SOMO (Figure 1), and the cyano carbon atom accordingly has a substantial fraction of the total unpaired spin density. For the η^2 structure the cyano carbon neither has significant spin density nor contributes to the SOMO.

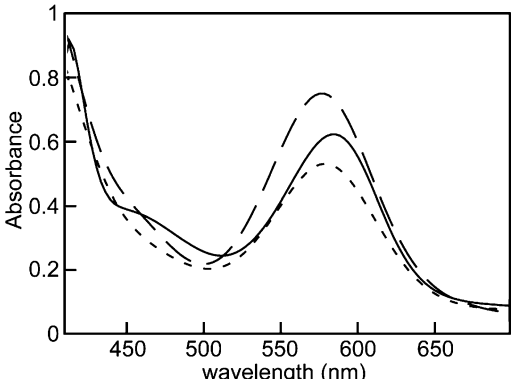

Figure 2. UV−vis spectra of ketimide complexes **3b** (Et_2O, 25 °C, long dashes), **3c** (Et_2O, 25 °C, short dashes), and **3d** (toluene, −40 °C, solid line).

We conclude that the η^1-benzonitrile bonding mode is the reactive form of system **5**. The buildup of radical character at the benzonitrile cyano carbon is what suggests the limiting molybdenum(IV) resonance structure **5b** in Scheme 2, with the molybdenum(III) resonance structure **5a** representing the other limit. In essence, back-bonding to the doubly degenerate π system of the η^1-bonded cyano function by the odd-electron d^3 molybdenum center necessarily confers radical character to the cyano carbon of the bound nitrile.

Interestingly, the computational analysis suggests that the odd-electron orbital for **5** is *in the same plane* as that defined by the benzonitrile phenyl ring, where it is relatively shielded from attack. This is consistent with the long lifetime and relatively slow dimerization process observed for **5**, and hence its utility as an easily trapped and persistent radical. This is in contrast with the observed very rapid dimerization of the less-shielded acetonitrile adduct of complex **1**.[28,34] The carbon-centered radical character of benzonitrile adduct **5** has led to its exploitation recently as a radical trap in remarkable heterobimetallic cross-couplings involving carbon dioxide, benzophenone, and pyridine.[35]

Synthesis of Ketimide Complexes 3. The new compounds **3b** and **3c** are generated quantitatively by simple addition to a solution of molybdenum(III) complex **1**, 1.0 equiv of PhCN followed by 0.5 equiv $C_6F_5EEC_6F_5$ (E = S and Se, respectively). This is as illustrated in Scheme 2. The asserted quantitative formation of **3b** and **3c** was confirmed by ^{1}H and ^{19}F NMR as well as UV−vis spectroscopies. Both **3b** and **3c** exhibit a characteristic distinctive blue-purple color corresponding to a strong (ϵ = ca. 5 × 10^3 M^{-1}cm^{-1}) absorption band at ca. 580 nm as shown in Figure 2.

The relative thermal stability of **3b** (X = SC_6F_5) permitted its isolation in 53% yield after recrystallization from ethyl ether. The molecular structure of **3b** as determined by single-crystal X-ray diffraction is presented in Figure 3 (see also Table 1). Multiple bonding between Mo1 and N4 is in evidence based on their 1.8082(16) Å interatomic distance. The N4−C41 unit should correspond to an imine-like C═N double bond functional group, but with its observed distance of 1.303(2) Å there is an elongation of ca. 0.01−0.03 Å as compared with typical imine

(33) Johnson, A. R.; Davis, W. M.; Cummins, C. C.; Serron, S.; Nolan, S. P.; Musaev, D. G.; Morokuma, K. *J. Am. Chem. Soc.* **1998**, *120*, 2071−2085.
(34) Tsai, Y. C.; Johnson, M. J. A.; Mindiola, D. J.; Cummins, C. C.; Klooster, W. T.; Koetzle, T. F. *J. Am. Chem. Soc.* **1999**, *121*, 10426−10427.
(35) Mendiratta, A.; Cummins, C. C. *Inorg. Chem.* **2005**, *44*, 7319−7321.

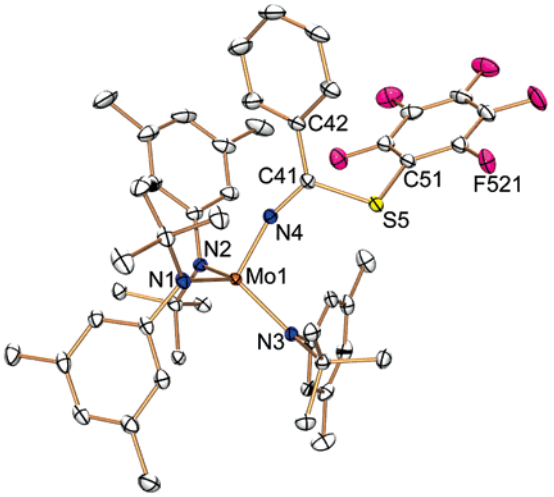

Figure 3. ORTEP rendering of ketimide complex **3b** with ellipsoids at the 50% probability level. Selected distances (Å) and angles (deg): Mo1−N4, 1.8082(16); N4−C41, 1.303(2); C41−S5, 1.790(2); S5−C51, 1.771-(2); Mo1−N4−C41, 162.03(14).

structures.[36,37] The corresponding value for **3e** (X = SC_6H_5) is 1.317(6) Å.[24] The slight C═N elongation relative to the typical imine function may reflect a hybridization at N4 closer to sp (cf. Mo1−N4−C41 = 162.03(14) °) together with back-bonding from the d^2 Mo center into the C═N π^* orbital. The S5−C51 separation of 1.771(1) Å is longer by ca. 0.03 Å than in H-bonded salts of the free $[SC_6F_5]^-$ anion,[38,39] but this may not be significant given that the S−C distance in di(pentafluorophenyl) sulfane is 1.752 Å.[40] Meanwhile, the C41−S5 distance of 1.790(2) Å is as expected for an sp^2 carbon atom bonded to an SC_6F_5 group.[41]

While **3b** (X = SC_6F_5) was stable enough for isolation and full characterization, selenium analogue **3c** (X = SeC_6F_5) could be generated similarly, but thermal instability obviated its isolation in pure form. Information on the benzonitrile extrusion kinetics for **3b** and **3c** is presented below.

Having successfully generated C−E (E = S and Se) single bonds by ostensible attack of a persistent carbon radical upon an E−E bonded system, we wondered if a C−O single bond might be available via attack of radical nitrile adduct **5** upon a peroxide. This was accomplished as shown in Scheme 3, in a manner very much analogous to the synthesis of **3b** and **3c**, with the distinction that of all the complexes **3a**−**f**, **3d** (X = O_2CPh) is by far the least thermally stable. The specific choice of benzoyl peroxide stemmed from our search for a group X that would beta eliminate with the greatest kinetic facility. If the mechanism of the beta-X elimination involves buildup of negative charge on X, then it would follow that X^- should be chosen such that it is a good leaving group.

When a thawing Et_2O solution (ca. −100 °C) of in situ generated **5** is combined with 0.5 equiv of benzoyl peroxide

Scheme 3

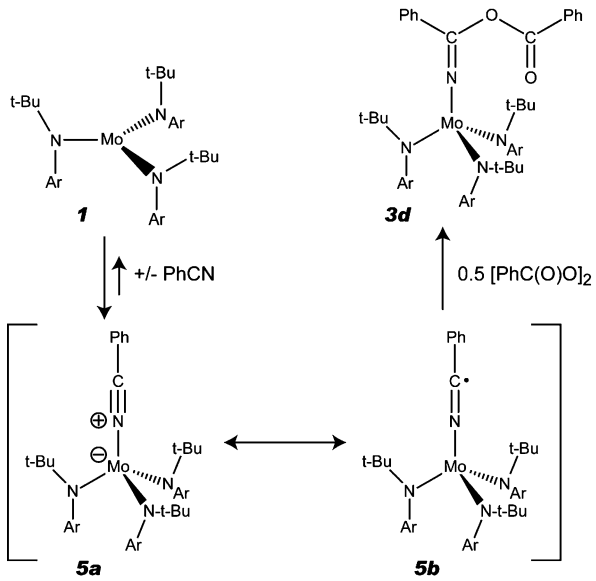

Scheme 4

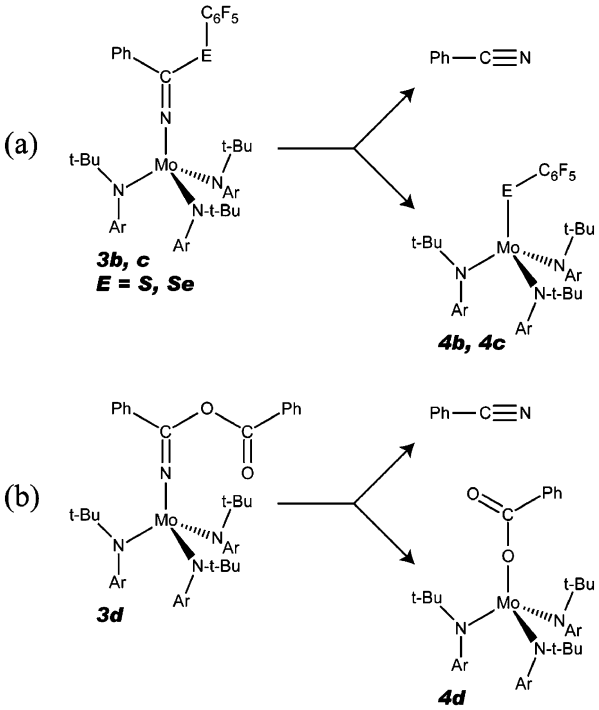

and then allowed to warm to room temperature, a sequence of color changes is observed as follows: purple → blue → purple. Assay of the crude reaction mixture by ^1H NMR spectroscopy reveals that molybdenum benzoate complex **4d** and PhC≡N are the exclusive products (Scheme 4b).

The Scheme 3 → Scheme 4b sequence could be monitored by ^1H NMR spectroscopy. Beginning the reaction of **5** with 0.5 equiv of benzoyl peroxide in thawing toluene-d_8 solution and then transferring the NMR tube containing the cold mixture to an NMR probe pre-cooled to −15 °C revealed clean formation of a system (assigned as blue **3d**) having a 2:1 ratio of N(*t*-Bu)Ar ligand environments along with two phenyl environments in a 1:1 ratio. With increasing temperature the 2:1 ratio of N(*t*-Bu)Ar ligand environments for **3d** becomes a single environment, and also the new resonances for **4d** and

(36) Tucker, P. A.; Hoekstra, A.; Tencate, J. M.; Vos, A. *Acta Crystallogr. B* **1975**, *B 31*, 733−737.
(37) Bokkers, G.; Kroon, J.; Spek, A. L. *Acta Crystallogr. B* **1979**, *35*, 2351−2354.
(38) Carmalt, C. J.; Dinnage, C. W.; Parkin, I. P.; White, A. J. P.; Williams, D. J. *Dalton* **2000**, 3500−3504.
(39) Chadwick, S.; Englich, U.; Noll, B.; Ruhlandt-Senge, K. *Inorg. Chem.* **1998**, *37*, 4718−4725.
(40) Minkwitz, R.; Preut, H.; Sawatzki, J. *Z. Anorg. Allg. Chem.* **1989**, *569*, 158−168.
(41) Abu Bakar, W. A. W.; Carlton, L.; Davidson, J. L.; Manojlovic-Muir, L.; Muir, K. W. *J. Organomet. Chem.* **1988**, *352*, C54−C58.

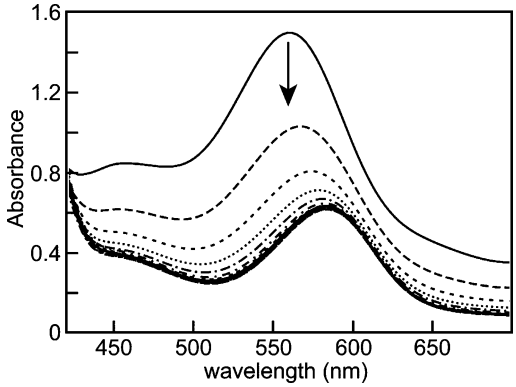

Figure 4. Spectral changes upon combining a premixed toluene solution of **1** (0.3 mM) and PhCN (0.45 mM) with a toluene solution of benzoyl peroxide (0.3 mM) in the stopped-flow apparatus at −80 °C. Total time: 15 s. The final spectrum is assigned to **3d**.

PhCN begin to appear. Finally, only the resonances for **4d** and PhCN remain.

Formation of **3d** according to Scheme 3 also was observed by the stopped-flow spectrophotometric method. As shown in Figure 4, when a premixed toluene solution of **1** and benzonitrile is combined with a benzoyl peroxide solution at −80 °C, conversion to ketimide **3d** is complete within 15 s. As shown in Figure 2, the spectrum obtained in this manner for **3d** compares well with those seen for the X = EC_6F_5 analogues **3b** and **3c**.

Also as observed by the stopped-flow spectrophotometric method, the PhCN adduct **5** is formed rapidly and quantitatively at low temperatures (−80 to −40 °C) when **1** is treated with a 10-fold excess of PhCN in toluene solution. The subsequent reaction of **5** with benzoyl peroxide giving **3d** is seen to follow clean second-order kinetics; the reaction is first order in complex **1** and first order in benzoyl peroxide. The reaction rate is independent of the PhCN concentration when excess PhCN is employed. For the **5** + 0.5 $[PhC(O)O]_2$ → **3d** reaction we obtain activation parameters of $\Delta H^{\ddagger} = 2.0 \pm 0.4$ kcal/mol and $\Delta S^{\ddagger} = -31 \pm 0.4$ eu from rate measurements made over the −80 to −40 °C temperature range (Figure S3). This compares well with activation parameters ($\Delta H^{\ddagger} = 3.7$ kcal/mol and $\Delta S^{\ddagger} = -29$ eu) reported previously[24] for the **5** + 0.5 PhTeTePh → **3a** reaction.

As will be discussed in more detail below in connection with the optimum procedures used for synthesizing the beta-elimination products **4b**-**4d** on a preparative scale, the direct reaction of complex **1** with benzoyl peroxide in the absence of PhCN does *not* smoothly yield **4d**. Studying the **1** + 0.5 $[PhC(O)O]_2$ reaction by the stopped-flow spectrophotometric method revealed it to be a slow second-order process with poorly reproducible kinetic behavior. An approximate activation enthalpy $\Delta H^{\ddagger} \approx 10 \pm 2$ kcal/mol was estimated for this reaction; see also Figure S4. While a detailed kinetic analysis was obviated for this direct reaction of **1** with benzoyl peroxide, it is of great interest that the reaction is much slower than is the case for nitrile adduct **5** reacting with the same substrate. With reference to the nitrile adduct **5** SOMO displayed in Figure 1, a possible explanation for the observed dichotomy is that nitrile binding to molybdenum(III) gives transmission of radical character to the cyano carbon which resides in a more substrate-accessible location. Furthermore, if radical attack upon benzoyl peroxide proceeds in two steps as follows:

$$\mathbf{5} + [PhC(O)O]_2 \rightarrow \mathbf{3d} + [PhCO_2\cdot] \quad \textit{slow} \qquad (1)$$

$$\mathbf{5} + [PhCO_2\cdot] \rightarrow \mathbf{3d} \quad \textit{fast} \qquad (2)$$

then we see that benzoyloxy radical capture would be a post-rate-determining step. In order for the overall process to be clean as observed, capture of the benzoyloxy radical (eq 2) must be an efficient process. If it is not, then products stemming from spontaneous decarboxylation of the benzoyloxy radical are expected to ensue.[42] It is possible that **1** itself is less efficient than **5** at capturing the intermediate benzoyloxy radical, accounting for the unclean overall direct reaction of **1** with benzoyl peroxide in the absence of PhCN.

Kinetics of Nitrile Extrusion. The process drawn in Scheme 4b and also represented here as eq 3, is the most facile of the nitrile-forming reactions discussed in the present work. Because the exotic intermediate ketimide complex **3d** and the molybdenum(IV) benzoate product **4d** both have prominent infrared spectroscopic features, the transformation of eq 3 was amenable to monitoring by continuous-flow infrared spectroscopy (Figure 5).

$$\mathbf{3d} \rightarrow \mathbf{4d} + \text{PhCN} \qquad (3)$$

Analysis of the intensity of the 1730 cm^{-1} band assigned to ketimide **3d** together with the 1660 cm^{-1} band assigned to benzoate **4d** as a function of time reveals clean first-order kinetic behavior (Figure S1). Rate constants were obtained in this manner over the temperature range −30 to 10 °C and are provided as Supporting Information. Activation parameters obtained from a fit of these rate constants (Figure S2) to the Eyring equation are as follows: $\Delta H^{\ddagger} = 18.6$ kcal/mol and $\Delta S^{\ddagger} = -0.1$ eu.

Elimination kinetics also were measured as a function of temperature for the X = EC_6F_5 derivatives **3b** and **3c**, in both cases by conventional diode-array UV−visible spectroscopy. The half-life of **3b** in THF solution at 25 °C was determined to be ca. 6.5 h. For **3b**, first-order rate constants were obtained over the temperature range 25−65 °C. Selenium derivative **3c** was substantially more thermally fragile than sulfur analogue **3b**, undergoing elimination with a half-life at 25 °C of ca. 6 min. Activation parameters along with thermodynamic data (discussed below) for the nitrile-forming elimination reactions probed herein are collected together in Table 2. With regard to solvent polarity effects, we note that the rate of the **3c** → **4c** + PhCN transformation was qualitatively the same in THF as in toluene solvent (^{1}H NMR observation).

As shown in Table 2 the highest activation enthalpy is for the SC_6F_5 derivative **3b** while the lowest is for the SeC_6F_5 system **3c**. A plausible mechanism for the nitrile extrusion reaction in these systems involves initial coordination of the S or Se atom to the molybdenum center with concomitant weakening of the E−C bond. Depicted in Chart 1 is the proposed transition structure ***TS1*** by which nitrile extrusion takes place for **3b** and **3c**; it is characterized by the formation of a congested four-membered ring structure. An alternative (less attractive) unimolecular mechanistic proposition would involve *heterolytic* E−C bond fragmentation as the initial step without any prior coordination of E to the molybdenum center.

(42) Chateauneuf, J.; Lusztyk, J.; Ingold, K. U. *J. Am. Chem. Soc.* **1988**, *110*, 2886−2893.

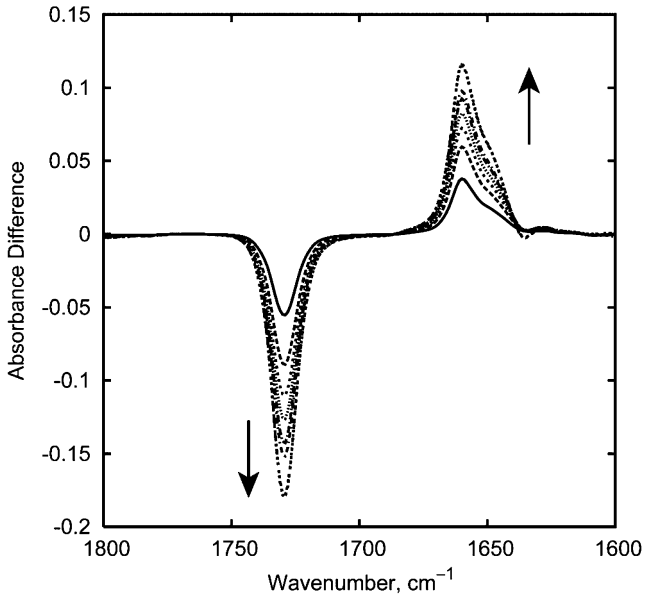

Figure 5. Vibrational spectroscopic monitoring of the **3d** → **4d** + PhCN transformation in toluene solution at 1.3 °C.

Table 2. Activation Parameters (kcal/mol and eu) and Thermodynamic Data (kcal/mol) for the Reaction **3** → **4** + PhCN, Where **3** = (Ar[*t*-Bu]N)$_3$Mo−N=C(X)Ph and **4** = (Ar[*t*-Bu]N)$_3$MoX

	$\Delta H^{\ddagger}$	$\Delta S^{\ddagger}$	ΔH^{o}
3b, X = SC_6F_5	22.5	−4.3	
3c, X = SeC_6F_5	16.5	−15.8	
3d, X = O_2CPh	18.6	−0.1	−2.4
3e, X = SPh			+10.0
3f, X = SePh			+5.8

Chart 1

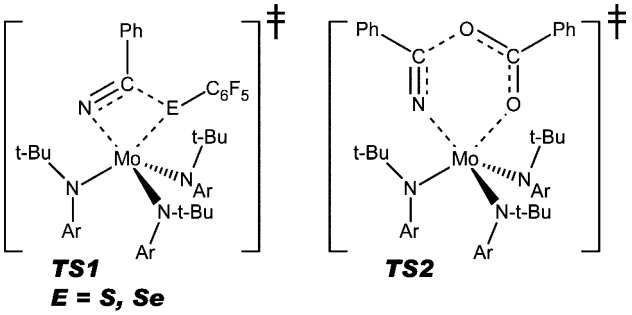

For fragmentation of the benzoyloxy-substituted ketimide derivative **3d**, a four-center mechanism such as that proposed for **3b** and **3c** is similarly consistent with the data in hand. In this case, however, it is important to note that an alternative six-membered ring transition structure ***TS2*** (Chart 1) is also possible.

From the foregoing mechanistic hypotheses we would predict that $\Delta H^{\ddagger}$ would, as observed, be lower for Se than for S following the E−C bond strength trend. In addition, the larger Se nucleus would increase crowding in transition state ***TS1***, resulting in a more negative $\Delta S^{\ddagger}$, as observed. The near-zero activation entropy for **3d** together with its relatively low enthalpy of activation is probably linked to its ability to form a less sterically hindered six-membered ring transition structure ***TS2***, as pointed out above. This may permit more complete establishment of the Mo−O bond concomitant with fission of the O−C bond.

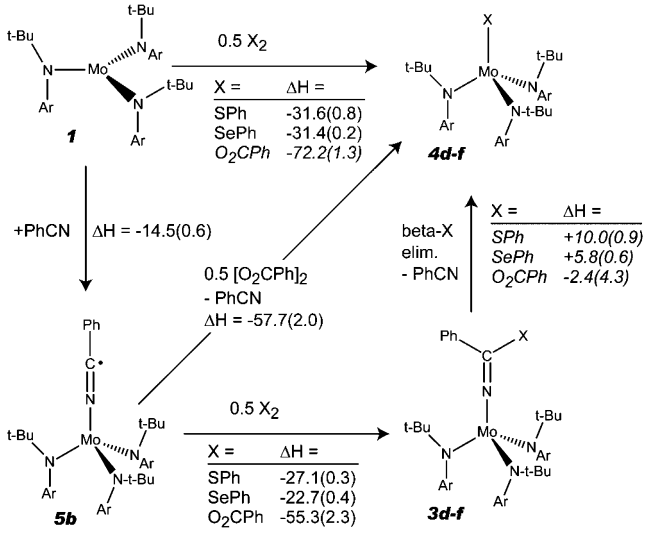

Figure 6. Thermodynamic data for enthalpies of reaction (kcal/mol) for the assembly of complexes **3d**−**f** and for nitrile extrusion giving **4d**−**f**. Experimental numbers are in roman font, while data calculated therefrom are italicized.

Thermodynamic Measurements. Thermochemical data for the ketimide **3d**−**f** formation reactions and for the formation reactions of molybdenum(IV) XMo(N[*t*-Bu]Ar)$_3$ (X = O_2CPh, **4d**; SPh, **4e**; and SePh, **4f**) complexes, both directly and via nitrile extrusion, are collected in Figure 6. The data for the direct reaction of **1** with 0.5 PhEEPh (E = S and Se, top of Figure 6) were reported by us previously.[24] Due to the fact that benzoyl peroxide does not cleanly react with **1** to produce **4d**, the value shown for this reaction is derived using Hess's law. The enthalpy of binding of benzonitrile to **1** giving adduct **5** has been independently determined by variable-temperature FTIR spectroscopy to be −14.5 ± 0.6 kcal/mol.[43] The enthalpy of reaction of adduct **5** with 0.5 PhEEPh yielding **3e**−**f** was measured during the first minute of reaction at +25 °C since **3e** and **3f** are essentially stable with respect to nitrile elimination at that temperature. For the reaction of **5** with benzoyl peroxide to give **3d**, however, subsequent PhCN extrusion to provide **4d** is rapid at +25 °C, and so this reaction enthalpy was measured at −25 °C. The thermodynamic measurements were performed in a low-temperature calorimetry system housed in an inert atmosphere glovebox as described in the Experimental Section.

Measurement of the enthalpy of reaction of **5** with benzoyl peroxide at +25 °C to give the benzoate molybdenum(IV) complex **4d** together with benzonitrile proceeded smoothly. This reaction is shown along the diagonal in Figure 6. These data permit calculation of enthalpies of benzonitrile extrusion as −2.4 ± 4.3, +5.8 ± 0.6, and +10.0 ± 0.9 respectively for X = O_2-Ph, SePh, and SPh. The order of exothermicities for PhCN elimination runs parallel to the observed kinetic stabilities; however, as discussed above, it is a complex mixture of enthalpy and entropy of activation that truly governs the PhCN elimination rate. For both X = SPh and SePh the elimination is endothermic. Accordingly, at a suitably low temperature the reverse reaction should become manifest if the kinetic barrier could be overcome at the lower temperatures required for PhCN insertion into the Mo−EPh bond to be spontaneous. These data

(43) Kryatova, O. P.; Rybak-Akimova, E. V.; Mendiratta, A.; Cummins, C. C.; McDonough, J. E.; Hoff, C. D. Manuscript in preparation.

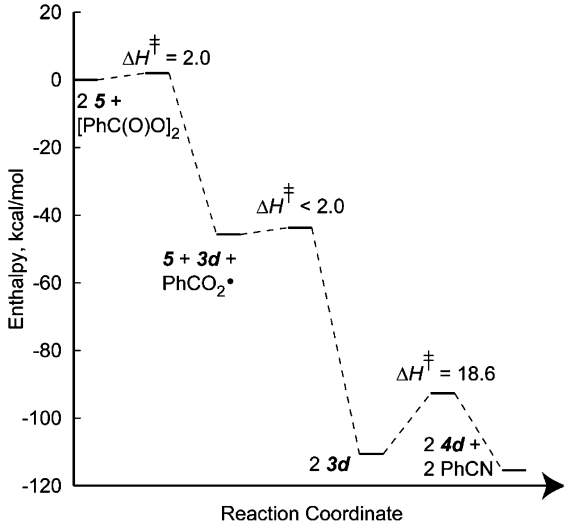

Figure 7. Potential energy diagram (enthalpies of reaction in kcal/mol) referenced to a zero point of 2 **5** + benzoyl peroxide. Data presented are a combination of thermodynamic and kinetic studies described in the text.

serve to illustrate the sensitivity of the nitrile elimination reaction to the balance of the C−E versus the Mo−E bond strengths.

The enthalpy of oxidation of **1** by 0.5 X_2 as in the top reaction of Figure 6 permits the generation of corresponding Mo−X bond strength estimates. It is noteworthy that reaction with benzoyl peroxide is more than twice as exothermic as is the oxidation with PhEEPh. Using respective values of 46, 41, and 19.2 kcal/mol for PhS−SPh,[44] PhSe−SePh,[44] and PhC(O)O−O(O)CPh[45] bond energies yields respective values of 55, 52, and 82 kcal/mol for the Mo−S, Mo−Se, and Mo−O bonds of **4e**, **4f**, and **4d**. It is interesting to compare these single-bond energy estimates with the multiple molybdenum(V) oxo and sulfido bond energies reported previously for EMo(N[*t*-Bu]Ar)$_3$: 156 and 104 kcal/mol for E = O and S, respectively.[33,46] Note that the metal−ligand multiple bonds are essentially twice as strong as corresponding single bonds to the same metal fragment.

The combination of thermodynamic and kinetic data from the present study yields the potential energy diagram of Figure 7. The first step is proposed to be the interaction of benzonitrile adduct **5** with benzoyl peroxide to generate benzoyloxy ketimide **3d** together with a free benzoyloxy radical [$PhCO_2$•]. This amounts to an SH2 mechansim.[47] A crucial and surprising feature of the potential energy diagram is the very low enthalpy of activation (ca. 2 kcal/mol) for this initial step, in effect the 1e C−O bond-forming oxidation of benzonitrile adduct **5** by benzoyl peroxide. This is a lower activation enthalpy than those observed for direct reactions of complex **1**, in which the unpaired spin density is metal-localized. Evidently the accumulation of unpaired spin density on the cyano carbon of benzonitrile adduct **5** translates into kinetically accelerated radical reactivity. Not to be discounted along these lines is the importance of transfer of unpaired spin density to a less sterically crowded site in adduct **5** as compared with starting metal complex **1** (cf. Figure 1). Thermodynamic and bond strength estimates discussed above indicate that production of a free benzoyloxy radical [$PhCO_2$•] by the initial interaction of PhCN adduct **5** with benzoyl peroxide is exothermic by ca. 46 kcal/mol. This stands as the most reasonable mechanism in accord with all data. The free radical [$PhCO_2$•] so generated is proposed to rapidly combine in a second step with a second equivalent of PhCN adduct **5**, giving a second equivalent of **3d**.

Synthesis and Molecular Structure of Molybdenum(IV) Benzoate 4d. The direct reaction of benzoyl peroxide with the three-coordinate molybdenum(III) complex **1** was not clean and thus not suitable for the synthesis of **4d**. Proton NMR analysis of crude reaction mixtures stemming from treatment of **1** with 0.5 equiv of benzoyl peroxide indicated ca. 30% yield of **4d** together with multiple unknown products among which was not the known oxo complex OMo(N[*t*-Bu]Ar)$_3$. Therefore, the alternative (quantitative) method of carrying out the benzoyloxylation reaction in the presence of PhCN was employed for the synthesis of pure **4d**. Paramagnetic benzoate **4d** was obtained by this method in 71% isolated yield as large brown crystals.

The oxidation of metal complexes by benzoyl peroxide as a route to metal benzoate derivatives has been employed by Legzdins to synthesize a bisbenzoate of vanadium from a corresponding dicarbonyl.[48] Digold(II) benzoate systems similarly have been obtained from digold(I) precursors by oxidation with benzoyl peroxide.[49] Reactions in which reducing metal systems bind organic nitriles (typically PhCN or MeCN) and effect bimetallic 2e reductive coupling of them are well-documented,[50] but cases in which the intermediate radical nitrile adduct is intercepted are rare. The titanium(III) complex Ti(N[*t*-Bu]Ar)$_2$(CH[$SiMe_3$]$_2$) reductively dimerizes PhCN, but in the presence of *t*-BuCN, to which it presumably binds, it abstracts N_3 radical from N_3SiMe_3.[51]

The molybdenum(IV) bisbenzoate complex $Cp_2Mo(O_2CPh)_2$ was synthesized by reaction of $Cp_2Mo(\eta^2$-NCMe)[52] with benzoyl peroxide, and notably, the same η^2-acetonitrile precursor also reacts smoothly with Et_2S_2 and Ph_2Se_2 to give molybdocene bis(ethylthiolate) and bis(phenylselenolate) complexes, respectively.[53] Bisbenzoate complex $Cp_2Mo(O_2CPh)_2$ was also the subject of a crystal and molecular structure investigation.[54] Thereby it was found that the independent benzoate ligands were bound η^1 with Mo−O−C angles (deg) of 131.0(4) and 128.6(4), and with Mo−O interatomic distances (Å) of 2.113(4) and 2.102(4).

In comparison with the latter the structure of molybdenum(IV) benzoate complex **4d** (Figure 8) is not remarkable except insofar as the Mo1−O4 distance of 2.0011(17) Å is shorter by ca. 0.1 Å, presumably indicative of greater O→Mo pπ donation. This is to be expected as the bisbenzoate $Cp_2Mo(O_2CPh)_2$ is an 18e system, while the Mo in **4d** has an empty dπ orbital

(44) McDonough, J. E.; Weir, J. J.; Carlson, M. J.; Hoff, C. D.; Kryatova, O. P.; Rybak-Akimova, E. V.; Clough, C. R.; Cummins, C. C. *Inorg. Chem.* **2005**, *44*, 3127−3136.
(45) Abel, B.; Assmann, J.; Botschwina, P.; Buback, M.; Kling, M.; Oswald, R.; Schmatz, S.; Schroeder, J.; Witte, T. *J. Phys. Chem. A* **2003**, *107*, 5157−5167.
(46) Cherry, J. P. F.; Johnson, A. R.; Baraldo, L. M.; Tsai, Y. C.; Cummins, C. C.; Kryatov, S. V.; Rybak-Akimova, E. V.; Capps, K. B.; Hoff, C. D.; Haar, C. M.; Nolan, S. P. *J. Am. Chem. Soc.* **2001**, *123*, 7271−7286.
(47) March, J. *Advanced organic chemistry: reactions, mechanisms, and structure*, 4th ed.; Wiley: New York, 1992.
(48) Hayton, T. W.; Patrick, B. O.; Legzdins, P. *Organometallics* **2004**, *23*, 657−664.
(49) Bennett, M. A.; Bhargava, S. K.; Hockless, D. C. R.; Welling, L. L.; Willis, A. C. *J. Am. Chem. Soc.* **1996**, *118*, 10469−10478.
(50) De Boer, E. J. M.; Teuben, J. H. *J. Organomet. Chem.* **1978**, *153*, 53−57.
(51) Johnson, A. R.; Davis, W. M.; Cummins, C. C. *Organometallics* **1996**, *15*, 3825−3835.
(52) Wright, T. C.; Wilkinson, G.; Motevalli, M.; Hursthouse, M. B. *Dalton Trans.* **1986**, 2017−2019.
(53) Deazevedo, C. G.; Carrondo, M.; Dias, A. R.; Martins, A. M.; Piedade, M. F. M.; Romao, C. C. *J. Organomet. Chem.* **1993**, *445*, 125−131.
(54) Carrondo, M.; Calhorda, M. J.; Hursthouse, M. B. *Acta Crystallogr. C* **1987**, *43*, 880−883.

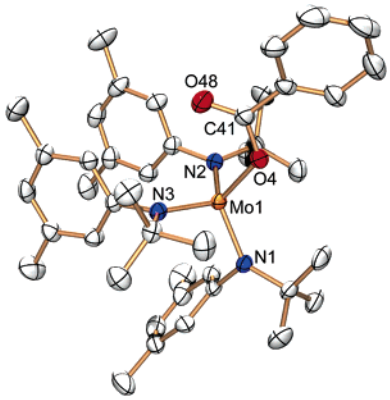

Figure 8. ORTEP rendering of one of two crystallographically independent molecules of benzoate complex **4d** with ellipsoids at the 50% probability level. Selected distances (Å) and angles (deg): Mo1−O4, 2.0017(13); Mo2−O8, 2.0126(14); C41−O4−Mo1 124.58(13); C81−O8−Mo2, 122.00(13); N2−Mo1−O4, 98.46(6); N3−Mo1−O4, 107.13(6); N1−Mo1−O4, 116.84(6).

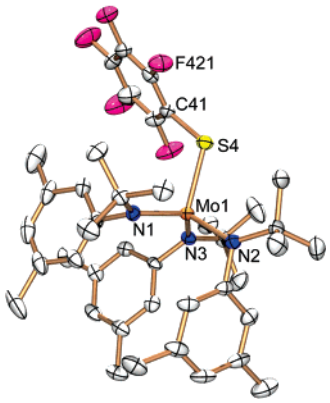

Figure 9. ORTEP rendering of pentafluorophenylthiolate complex **4b** with ellipsoids at the 50% probability level. Selected distances (Å) and angles (deg): Mo1−S4, 2.3087(11); S4−C41, 1.783(4); C41−S4−Mo1, 115.05(14); Mo1−N1, 1.939(3); Mo1−N3, 1.945(3); Mo1−N2, 1.979(3).

prepared to accept donation from a benzoate oxygen lone pair in the plane perpendicular to the Mo1−O4−C41 bend angle. While **4d** exhibits paramagnetism in solution according to its ^{1}H NMR spectroscopic data, it is likely diamagnetic in the solid state based upon the observed pseudo-C_s conformation of ancillary *N*-*tert*-butylanilide ligands. This behavior, indicative of a small singlet−triplet gap, is identical to that observed previously for the molybdenum(IV) iodide complex IMo(N[*t*-Bu]Ar)$_3$.[55]

It is not known whether the reaction of benzoyl peroxide with Cp$_2$Mo(η^2-NCMe) to yield bisbenzoate Cp$_2$Mo(O$_2$CPh)$_2$ proceeds via a benzoyloxy ketimide species analogous to **3d**.

Synthesis of Molybdenum(IV) Chalcogenolates 4b and 4c. Obtained in 57 and 54% yields (following recrystallization) respectively upon addition of 0.5 equiv of $C_6F_5EEC_6F_5$ to three-coordinate **1** are the molybdenum(IV) (C_6F_5E)Mo(N[*t*-Bu]Ar)$_3$ complexes **4b** and **4c**, where E = S and Se, respectively. The reactions are carried out in Et$_2$O in which solvent the reaction mixtures take on a purple-brown color upon mixing at 25 °C. While ^{1}H NMR spectroscopic interrogation of crude reaction mixtures suggests quantitative formation of **4b** and **4c**, their isolated yields are lower due to losses incurred during purification and have not been optimized. The NMR spectroscopic data for **4b** and **4c** further suggest that these complexes, unlike benzoate **4d**, are diamagnetic in solution. Thus, they are predicted to possess a larger singlet−triplet energy gap and a more significant p$\pi \rightarrow$ dπ Mo−E interaction. In fact, given the isolobal nature of ER (E = S, Se) and NR$_2$ as single π-face monoanions, it can be appreciated that **4b** and **4c** are isolobal to the iconic Mo(NMe$_2$)$_4$ molecule which similarly is purple and diamagnetic.[56,57]

Molybdenum pentafluorophenylthiolate complexes are not exceptionally numerous, but they have been of interest as metalloligands.[58−64] The complex CpMo(O)(CF_3CCCF_3)(SC_6F_5), nominally a molybdenum(IV) example, is associated with an Mo−S distance of 2.402 Å and Mo−S−C angle of 107.77°.[65] The latter parameters are respectively greater and smaller than corresponding parameters obtained in the present work for complex **4b** (see caption to Figure 9). That the Mo−S distance should be smaller for **4b** is consistent with the optimal situation therein for formation of an Mo−S π bond via sulfur lone pair donation. Also, the relatively crowded nature of **4b** accounts for its more open Mo−S−C angle.

Concluding Remarks

Radical character of the cyano carbon atom of benzonitrile bound to molybdenum(III) has been found to provide a low-energy and efficient pathway for the generation of molybdenum(IV) ketimide complexes (Ar[*t*-Bu]N)$_3$Mo−N=C(X)Ph (X = EPh, EC_6F_5, or O$_2$CPh). Kinetic studies of formation of featured benzoyloxyketimide intermediate **3d** support a S$_H$2 mechanism for this process in which benzoyl peroxide is attacked by the bound nitrile and the O−O bond is ruptured, with [•O$_2$CPh] being trapped by a second equivalent of nitrile adduct **5** in a post rate-determining step.

The ketimide intermediates **3b**−**d** undergo subsequent quantitative PhC≡N extrusion by a unimolecular mechanism in what is a nearly thermoneutral process. In the case of X = O$_2$CPh the benzonitrile extrusion reaction has been found to be both facile and enthalpically downhill. Nitrile extrusion is somewhat less kinetically facile for X = SC_6F_5 and SeC_6F_5, such that intermediate **3b** (X = SC_6F_5) was sufficiently stable for structural characterization by X-ray crystallography. Nitrile extrusion is enthalpically uphill in the case of the less electron-withdrawing X = SPh or SePh substituents.

Nitrile complexes of type **5** challenge conventional views of oxidation state and are best viewed as adducts of bound organic radicals as illustrated by the graphical depiction of the SOMO for model system **5miii** (Figure 1). This work presents physical

(55) Peters, J. C.; Baraldo, L. M.; Baker, T. A.; Johnson, A. R.; Cummins, C. C. *J. Organomet. Chem.* **1999**, *591*, 24−35.
(56) Bradley, D. C.; Chisholm, M. H. *J. Chem. Soc., A* **1971**, 2741−4.
(57) Chisholm, M. H.; Cotton, F. A.; Extine, M. W. *Inorg. Chem.* **1978**, *17*, 1329−1332.
(58) Davidson, J. L.; Holz, B.; Lindsell, W. E.; Simpson, N. J. *Dalton Trans.* **1996**, 4011−4017.
(59) Davidson, J. L.; Lindsell, W. E.; McCullough, K. J.; McIntosh, C. H. *Organometallics* **1995**, *14*, 3497−3506.
(60) Davidson, J. L.; McIntosh, C. H.; Leverd, P. C.; Lindsell, W. E.; Simpson, N. J. *Dalton Trans.* **1994**, 2423−2429.
(61) Boyd, A. S. F.; Davidson, J. L.; McIntosh, C. H.; Leverd, P. C.; Lindsell, W. E.; Simpson, N. J. *Dalton Trans.* **1992**, 2531−2532.
(62) Abu Bakar, W. A. W.; Davidson, J. L.; Lindsell, W. E.; McCullough, K. J. *Dalton Trans.* **1990**, 61−71.
(63) Abu Bakar, W. A. W.; Davidson, J. L.; Lindsell, W. E.; McCullough, K. J.; Muir, K. W. *Dalton Trans.* **1989**, 991−1001.
(64) Abu Bakar, W. A. W.; Davidson, J. L.; Lindsell, W. E.; Muir, K. W. *J. Organomet. Chem.* **1987**, *322*, C1−C6.
(65) Howard, J. A. K.; Stansfield, R. F. D.; Woodward, P. *Dalton Trans.* **1976**, 246−250.

studies in which the MoN═C(•)Ph radicals are initially oxidized at the C-based radical forming MoN═C(X)Ph ketimides. The oxidative reactions are cleaner and faster when taking place at the C-based radical than at the metal center itself. Subsequent migration of the β-X group to the metal with PhC≡N extrusion depends markedly on the nature of the X group, but is relatively fast for X = O_2CPh, a finding attributed to the potential for a six-membered chelate transition structure.

Although the intermediates undergoing nitrile extrusion have herein been obtained by a process of radical nitrile incorporation, a clear view is obtained of chemistry that might alternatively be entered into by formal carbene, e.g. [**:**C(X)Ph], transfer to a terminal nitrido complex. The facile nature of the organic nitrile extrusion process provides the potential for development of new pathways for stoichiometric, and possibly catalytic, incorporation of N atoms from metal nitrido complexes into organic nitrogen compounds.

Acknowledgment. We thank the U.S.A. National Science Foundation for funding via CRC-0209977, and C.C.C. gives additional thanks for funding via CHE-0316823.

Supporting Information Available: Rate constants, kinetic and Eyring plots, CIF files corresponding to crystallographic structure determinations, computational details and coordinate files in xyz format for the computationally optimized structures of **5mi**−**5miii**. This material is available free of charge via the Internet at http://pubs.acs.org.

JA0587796